

Virtual Optical Network Embedding (VONE) Over Elastic Optical Networks

Long Gong, *Student Member, IEEE*, and Zuqing Zhu, *Senior Member, IEEE*

Abstract—Based on the concept of infrastructure as a service, optical network virtualization can facilitate the sharing of physical infrastructure among different users and applications. In this paper, we design algorithms for both transparent and opaque virtual optical network embedding (VONE) over flexible-grid elastic optical networks. For transparent VONE, we first formulate an integer linear programming (ILP) model that leverages the all-or-nothing multi-commodity flow in graphs. Then, to consider the continuity and consecutiveness of substrate fiber links' (SFLs') optical spectra, we propose a layered-auxiliary-graph (LAG) approach that decomposes the physical infrastructure into several layered graphs according to the bandwidth requirement of a virtual optical network request. With LAG, we design two heuristic algorithms: one applies LAG to achieve integrated routing and spectrum assignment in link mapping (i.e., *local resource capacity (LRC)-layered shortest-path routing LaSP*), while the other realizes coordinated node and link mapping using LAG (i.e., *layered local resource capacity (LaLRC)-LaSP*). The simulation results from three different substrate topologies demonstrate that *LaLRC-LaSP* achieves better blocking performance than *LRC-LaSP* and an existing benchmark algorithm. For the opaque VONE, an ILP model is also formulated. We then design a LRC metric that considers the spectrum consecutiveness of SFLs. With this metric, a novel heuristic for opaque VONE, *consecutiveness-aware LRC-K shortest-path-first fit (CaLRC-KSP-FF)*, is proposed. Simulation results show that compared with the existing algorithms, *CaLRC-KSP-FF* can reduce the request blocking probability significantly.

Index Terms—Elastic optical networks (EONs), network virtualization, virtual optical network embedding (VONE).

I. INTRODUCTION

RECENTLY, in order to adapt to the booming of Internet-based applications, researchers have proposed to utilize network virtualization as a solution to overcome the ossification of the current Internet infrastructure [1]. Meanwhile, the rapid growth of Internet traffic has been stimulating the research and development on optical transmission and switching technologies, for scaling metro and core networks cost-effectively. One famous example is the introduction of the flexible-grid elastic optical networks (EONs) [2]. With technologies such as the

optical orthogonal frequency-division multiplexing, EONs allow the optical spectra to be allocated at the granularity of a few gigahertz or even lower, which facilitates agile spectrum management in the optical layer. Therefore, flexible-grid elastic optical networking has been considered as a promising enabling technology for the physical infrastructure of the next generation Internet [2].

Based on the concept of infrastructure as a service, optical network virtualization facilitates the sharing of physical infrastructure among different users and applications, and enables network operators to efficiently offer their network resources as a service [3], [4]. Specifically, a virtual optical network (VON) can be constructed for each infrastructure renter (user) or application, and multiple VONs share the computing, switching and bandwidth resources in the same physical infrastructure [5]. A VON is composed of several virtual nodes (VNs) interconnected by virtual optical links (VOLs). Typically, a network operator constructs VONs using virtual optical network embedding (VONE), which allocates necessary resources in the physical infrastructure to each VON through node mapping and link mapping. Due to its complexity, VONE has become a major challenge for optical network virtualization [6]. Even though VONE over fixed-grid wavelength-division multiplexing (WDM) networks has been studied extensively [6]–[9], VONE over flexible-grid EONs has just started to attract research interests [10]–[12]. Because there are additional constraints, the problem is more complicated.

It is known that VONE can be classified into offline (or static) and online (or dynamic) problems [13]. The offline VONE addresses the schemes where all the VON requests are known *a priori*, while in the online one, the VON requests can come in and leave dynamically and are not known before their arrivals. On the other hand, if we consider whether the connections in a VON can be set up all-optically in the substrate network, we can categorize VONE into transparent and opaque scenarios. For the transparent VONE, we assume that there are no all-optical or optical-to-electrical-to-optical (O/E/O) spectrum converters in the substrate network. Therefore, to ensure all the connections in a VON can be established all-optically, we need to make sure that all the VOLs in a VON use the same spectrum on substrate fiber links (SFLs), which is also the assumption in previous work on transparent VONE [6], [12]. On the contrary, the opaque VONE only applies the spectrum continuity constraint to each VOL¹.

¹Note that in this study, we only allow a VOL to be embedded all-optically, i.e., for both transparent and opaque VONE, the link mapping has to make sure that a VOL uses the same optical spectrum on all of its substrate links. and the connections in a VON may be established opaquely in the substrate network.

Manuscript received August 24, 2013; revised October 23, 2013; accepted December 5, 2013. Date of publication December 5, 2013; date of current version December 25, 2013. This work was supported in part by the National Council for Educational Technology Project NCET-11-0884, the Natural Science Foundation of China Project 61371117, in part by the Fundamental Research Funds for the Central Universities (WK2100060010), and in part by the Strategic Priority Research Program of the Chinese Academy of Sciences (XDA06010301).

The authors are with the School of Information Science and Technology, University of Science and Technology of China, Hefei, Anhui 230027, China (e-mail: gonglong@mail.ustc.edu.cn; zqzhu@ieec.org).

Color versions of one or more of the figures in this paper are available online at <http://ieeexplore.ieee.org>.

Digital Object Identifier 10.1109/JLT.2013.2294389

In this paper, we investigate algorithms for both transparent and opaque VONE over flexible-grid EONs. For transparent VONE, we first formulate an integer linear programming (ILP) model that leverages the all-or-nothing multi-commodity flow in graphs. Then, to consider the continuity and consecutiveness of SFLs' optical spectra, we propose a layered-auxiliary-graph (LAG) approach that decomposes the physical infrastructure into several layered graphs according to the bandwidth requirement of a VON request. With this approach, we design two heuristic algorithms: one applies LAG to achieve integrated routing and spectrum assignment (RSA) in link mapping, while the other realizes coordinated node and link mapping using LAG. For the opaque VONE, we also first formulate an ILP, but with a path-based model. Then, we design a local resource capacity (LRC) metric that considers the spectrum consecutiveness of SFLs. Based on it, a novel heuristic for opaque VONE is proposed.

The remainder of the paper is organized as follows. Section II surveys the related work on VONE. The network models and problem descriptions of transparent and opaque VONE over EONs are provided in Section III. Sections IV and V-A discuss the ILP models, the heuristics and the performance evaluations of transparent and opaque VONE, respectively. Finally, Section VI summarizes the paper.

II. RELATED WORK

Virtual optical network embedding (VONE) realizes resource allocation for optical network virtualization. Similar to its counterpart for Layer 2/3 network virtualization, VONE generally consists of two stages, node mapping and link mapping. Most of the previous studies on VONE were targeted for fixed-grid WDM networks. Assuming that all the substrate nodes (SNs) were equipped with sufficient wavelength converters, Zhang *et al.* formulated a mixed ILP model and proposed two greedy heuristics for offline VONE in WDM networks in [7]. However, since the proposed heuristics perform node mapping and link mapping separately, coordinated VONE may not be achieved and there is still margin for performance improvements. In [8], Peng *et al.* considered the physical layer impairments (PLIs) and designed algorithms to achieve online PLI-aware VONE in WDM networks. Focusing on link mapping, Pages *et al.* formulated ILP models for opaque and transparent VONE in WDM networks in [6]. Note that the investigations in [6] and [8] did not consider node mapping in VONE. Several heuristic algorithms were laid out in [9] to jointly consider the node and link mapping of opaque VONE in WDM networks.

Recent studies have suggested that optical network virtualization over flexible-grid EONs can potentially provide efficient support to emerging cloud services, especially for the highly-distributed and data-intensive applications such as petabits-scale grid computing [2]–[4]. The operation principles and key enabling technologies for this type of optical network virtualization were reviewed in [3] and [4]. The reviews pointed out that the bandwidth-variable transponders require a VOL to use frequency slots (FS') that are spectrally contiguous. Hence, the

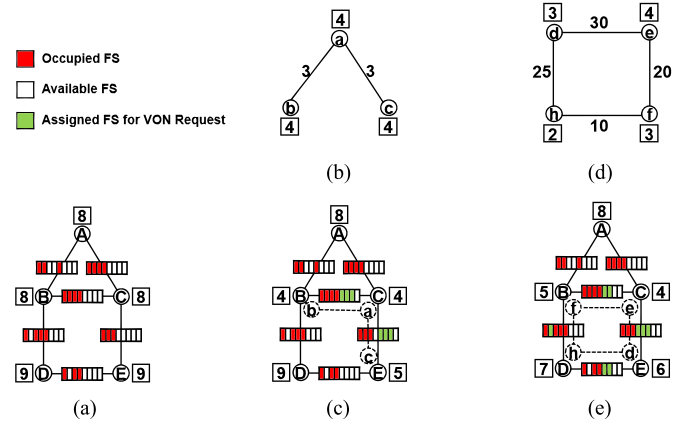


Fig. 1. Examples of the transparent and opaque VONE. (a) Substrate EON. (b) Transparent VON request. (c) Transparent VONE result. (d) Opaque VON request. (e) Opaque VONE result.

corresponding VONE needs to deal with additional constraints, which make the algorithms developed for VONE in WDM networks not directly applicable. In [10], Pages *et al.* considered link mapping in EONs but did not address flexible node mapping. An ILP model and two heuristics for the opaque VONE over EONs were proposed in [11], where the authors assumed that multiple VNs could be mapped onto the same SN. This assumption, however, limits the practicalness of the VONE algorithms, especially for the situations where the bandwidth requirement between VNs is too large for the internal channels of a SN. Moreover, some VONE schemes require location-constrained node mapping or high availability of the VON [14], which can also make mapping multiple VNs to the same SN not feasible.

III. PROBLEM DESCRIPTIONS

A. Network Model

In this study, we model the substrate EON as an undirected graph, denoted as $G^s(V^s, E^s)$, where V^s is the set of SNs, and E^s represents the set of SFLs. Each SN $v^s \in V^s$ has a computing capacity of $c_{v^s}^s$. Based on the operation principle of EONs [2], [15], we assume that each SFL $e^s \in E^s$ can accommodate B^s FS'. Fig. 1(a) illustrates an example of the substrate EON, where the numbers in the boxes around the SNs (A–E) are their computing capacities, and the slots on each SFL corresponds to its spectrum utilization. We can define a bit-mask $b_{e^s}^s$ that contains B^s bits to describe the spectrum utilization of an SFL e^s , i.e., $b_{e^s}^s[j] = 1$ indicates that the j th FS on e^s is occupied, otherwise, $b_{e^s}^s[j] = 0$. With $b_{e^s}^s$, we obtain two important parameters of the spectrum utilization: $w_{e^s}^s$ and $z_{e^s}^s$, which denote the starting and ending FS indices of the maximal contiguous slot-blocks (MCSBs) on e^s . Fig. 2 shows an example of the MCSBs on a SFL.

Definition 1: A contiguous slot-block (CSB) is a block of one or more FS' that are available and contiguous in the spectrum domain.

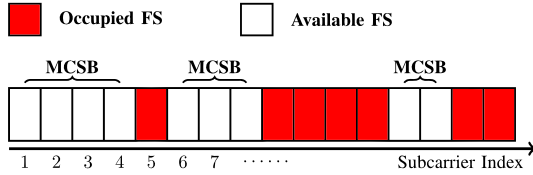


Fig. 2. An example of the MCSBs on an SFL.

Definition 2: A MCSB is a CSB that includes all the available and contiguous FS(s) at a spectral location.

B. VONE Process

Similar to the substrate topology, a VON request can also be modeled as an undirected graph $G^r(V^r, E^r)$, where V^r is the set of VNs, and E^r represents the set of VOLs. Each VN $v^r \in V^r$ associates with a computing resource requirement $c_{v^r}^r$, while the bandwidth requirement of each VOL $e^r \in E^r$ is $\text{bw}_{e^r}^r$ (in terms of Gb/s). In this study, we consider both node mapping and link mapping in the VONE process. In the node mapping, each VN from the VON request is mapped onto a unique SN that has sufficient computing capacity.² The link mapping is essentially a special RSA operation. Specifically, the RSA sets up a lightpath in the physical infrastructure for each VOL to satisfy its bandwidth requirement, under the spectrum non-overlapping, continuity and contiguous constraints [12].

1) *Transparent VONE:* As we have explained in Section I, the transparent VONE needs to make sure that all the VOLs in a VON use the same spectrum on SFLs. More specifically, the CSBs allocated to all the VOLs in a VON request should be the same in terms of indices. Hence, the bandwidth requirements of all the VOLs are the same in a VON request, and for simplicity, we denote them as n^r in terms of FS' (i.e., $\text{bw}_{e^r}^r = n^r \cdot C_{\text{FS}}$, where C_{FS} is the capacity of a single FS). Fig. 1(b) shows a transparent VON request, where the numbers in the boxes around the VNs are their computing resource requirements and the numbers on the VOLs are the bandwidth requirements n^r . Fig. 1(c) shows the VONE result in the substrate network after embedding the VON request in Fig. 1(b) successfully. The node mapping is $\{a \rightarrow C, b \rightarrow B, c \rightarrow E\}$, while the link mapping is $\{(a, b) \rightarrow (C, B), (a, c) \rightarrow (C, E)\}$ with the assigned CSB highlighted as green slots.

2) *Opaque VONE:* Different from the transparent one, the opaque VONE only needs to confirm that all the SFLs of a VOL use the same spectrum, i.e., the lightpath in the physical infrastructure for a VOL is set up under the spectrum continuity constraint. Therefore, the bandwidth requirements of the VOLs in a VON can be different and each VOL can be allocated to different CSBs with different modulation-levels. Fig. 1(d) shows an opaque VON request, where the computing resource and bandwidth requirements are labeled similarly as in Fig. 1(b), with the only difference that the bandwidth requirements are in terms of gigabyte per second.

²Note that in this study, we only consider one-to-one node mapping, i.e., VN splitting and VN merging are not allowed in the node mapping.

The opaque VONE result is shown in Fig. 1(e). The node mapping is $\{d \rightarrow E, e \rightarrow C, f \rightarrow B, h \rightarrow D\}$, and the link mapping is $\{(d, e) \rightarrow \{(E, C), 4-6\}, (e, f) \rightarrow \{(C, B), 5-6\}, (f, h) \rightarrow \{(B, D), 2-2\}, (h, d) \rightarrow \{(D, E), 5-6\}\}$.

Here, the link mapping result is denoted differently from that of the transparent VONE. On the right side of the arrow, the first term is the substrate lightpath, and the second one shows the starting and ending FS indices of the assigned CSB. Note that in this example, for simplicity, we assume that the modulation-levels for all the VOLs are BPSK, and a single BPSK FS can carry 12.5 Gb/s capacity. More details about how to determine the modulation-levels would be explained in Section V-A.

IV. TRANSPARENT VONE OVER EONS

A. ILP Formulation

In this section, we formulate an ILP model for transparent VONE over EONS. The ILP formulation is inspired by the all-or-nothing multi-commodity flow problem [16], and its details are as follows.

Parameters:

- 1) $G^s(V^s, E^s)$ Substrate topology of the physical infrastructure.
- 2) $c_{v^s}^s$ Computing capacity of each SN $v^s \in V^s$.
- 3) B^s Total number of FS' on each SFL $e^s \in E^s$.
- 4) $w_{(u^s, v^s), k}^s$ Starting FS index of the k th MCSB on the SFL $e^s = (u^s, v^s)$.
- 5) $z_{(u^s, v^s), k}^s$ Ending FS index of the k th MCSB on the SFL $e^s = (u^s, v^s)$.
- 6) $G^r(V^r, E^r)$ The VON request.
- 7) $s_{e^r}^r / d_{e^r}^r$ End-nodes of the VOL $e^r \in E^r$.
- 8) $c_{v^r}^r$ Computing resource requirement of the VN $v^r \in V^r$.
- 9) n^r Bandwidth requirement of each VOL in the VON.

Variables:

- 1) ξ_{v^r, v^s} Boolean variable that equals 1, if the VN v^r is mapped onto the SN v^s , otherwise, $\xi_{v^r, v^s} = 0$.
- 2) $f_{u^s, v^s}^{e^r}$ Boolean all-or-nothing flow variable that equals 1 if the all-or-nothing flow is on the SFL $e^s = (u^s, v^s)$ for the VOL $e^r \in E^r$, otherwise, it is 0.
- 3) $\delta_{(u^s, v^s)}^{(k)}$ Boolean variable that equals 1, if a CSB in the k th MCSB on the SFL $e^s = (u^s, v^s)$ is assigned to the VON request $G^r(V^r, E^r)$, otherwise, it is 0.
- 4) w Integer variable that indicates the starting FS index of the CSB assigned to the VON request $G^r(V^r, E^r)$.
- 5) z Integer variable that indicates the ending FS index of the CSB assigned to the VON request $G^r(V^r, E^r)$.

Objective:

$$\text{Minimize } w + B^s \cdot \sum_{e^r \in E^r} \sum_{(u^s, v^s) \in E^s} f_{u^s, v^s}^{e^r}. \quad (1)$$

With the objective in (1), we aim to minimizing the total number of used FS' for the VON request as well as the starting FS index of the assigned CSB.

Constraints:

1) Node mapping,

$$\sum_{v^s \in V^s} \xi_{v^r, v^s} = 1, \quad \forall v^r \in V^r \quad (2)$$

$$\sum_{v^r \in V^r} \xi_{v^r, v^s} \leq 1, \quad \forall v^s \in V^s. \quad (3)$$

Equations (2)–(3) ensure that each VN in the VON request is mapped onto a unique SN,

$$\sum_{v^s \in V^s} \xi_{v^r, v^s} \cdot c_{v^s}^s \geq c_{v^r}^r, \quad \forall v^r \in V^r. \quad (4)$$

Equation (4) ensures that the embedded SN has enough computing capacity to accommodate the VN.

2) Link mapping,

$$\sum_{(u^s, v^s) \in E^s} f_{u^s, v^s}^{e^r} - \sum_{(v^s, u^s) \in E^s} f_{v^s, u^s}^{e^r} = \xi_{s_{e^r}, u^s}^r - \xi_{d_{e^r}, u^s}^r \\ \forall e^r \in E^r, \forall u^s \in V^s. \quad (5)$$

Equation (5) is the flow conservation constraint. This constraint ensures that on all the SNs, the total number of the in-flows equals to that of the out-flows, except for the embedded SNs for the end-nodes of the VOL:

$$\sum_{e^r \in E^r} (f_{u^s, v^s}^{e^r} + f_{v^s, u^s}^{e^r}) \leq 1, \quad \forall (u^s, v^s) \in E^s. \quad (6)$$

Equation (6) ensures that for all the VOLs, their embedded lightpaths in the substrate topology are link-disjoint:

$$z - w + 1 = n^r. \quad (7)$$

Equation (7) ensures that the size of the assigned CSB for the VON request can satisfy its bandwidth requirement:

$$\sum_k \delta_{(u^s, v^s)}^{(k)} = \sum_{e^r \in E^r} (f_{u^s, v^s}^{e^r} + f_{v^s, u^s}^{e^r}), \quad \forall (u^s, v^s) \in E^s \quad (8)$$

$$w \geq z_{(u^s, v^s), k}^s \cdot \delta_{(u^s, v^s)}^{(k)}, \quad \forall (u^s, v^s) \in E^s, \forall k \quad (9)$$

$$z \leq (z_{(u^s, v^s), k}^s - B^s) \cdot \delta_{(u^s, v^s)}^{(k)} + B^s \\ \forall (u^s, v^s) \in E^s, \forall k. \quad (10)$$

Equations (8)–(10) make sure that the assigned CSB for $G^r(V^r, E^r)$ is located in a single MCSB on the SFLs, and the size of the MCSB is bigger than or equal to that of the assigned CSB.

3) Variable range:

$$\xi_{v^r, v^s} \in \{0, 1\}, \quad \forall v^r \in V^r, v^s \in V^s \quad (11)$$

$$f_{u^s, v^s}^{e^r}, \delta_{(u^s, v^s)}^{(k)} \in \{0, 1\}, \quad \forall (u^s, v^s) \in E^s, \forall e^r \in E^r, \forall k \quad (12)$$

$$w, z \in [1, B^s]. \quad (13)$$

Equations (11)–(13) limit the ranges of the variables.

Algorithm 1: LAG Construction

input : $G^s(V^s, E^s)$, n^r , k as the LAG's index
output: G_k^{sub} as the k -th LAG

- 1 $G_k^{sub} = G^s$;
- 2 mark the bandwidth on all the SFLs in G_k^{sub} as n^r ;
- 3 **for** all $e^s \in E^s$ in G^s **do**
- 4 **if** $\sum_{j=k}^{k+n^r-1} b_{e^s}^s[j] > 0$ **then**
- 5 | remove the SFL e^s in G_k^{sub} ;
- 6 **end**
- 7 **end**

B. Heuristic Algorithms

In this section, we propose two heuristic algorithms for the transparent VONE. Both of the algorithms are based on a LAG approach, which decomposes the substrate network into several layered graphs according to the bandwidth requirement of the VON request.

1) *LAG Approach*: For a VON request, $G^r(V^r, E^r)$, we first convert its bandwidth requirement $bw_{e^r}^r$ to the number of required FS' n^r , according to the bandwidth of the FS and the modulation-level supported in the substrate network. Then, by scanning the spectrum utilization of all the SFLs, we decompose the substrate topology into several layers. Specifically, for the k th layer, the LAG approach checks whether the CSB covering k th to $(k + n^r - 1)$ th FS' exists on each SFL $e^s \in E^s$. If the CSB exists on an SFL e^s , e^s is inserted into the k th layer, denoted as G_k^{sub} . Algorithm 1 explains the details of the LAG approach.

2) *Node Mapping*: It is known that for network virtualization, the node mapping can be achieved with the aid of the LRC [17]. We therefore consider to modify the definition of the LRC for Layer 2/3 network virtualization and adapt it to our VONE problem. In order to investigate the performance of the node mapping, we come up with two definitions as follows.

Definition 3: For a topology $G(V, E)$ in which the computing capacity of a node v is c_v , and the bandwidth capacity of a link e is bw_e , the LRC of node v is defined as follows Note that this definition works for both the substrate network and the VON requests. For VON requests, the resource capacities should be replaced by the corresponding resource requirements³:

$$h_v^{(1)} = c_v \cdot \sum_{(v, u) \in E} bw_{(v, u)}, \quad \forall v \in V. \quad (14)$$

Note that, in the k th layer LAG G_k^{sub} , the node computing capacities equal to those in the substrate topology $G^s(V^s, E^s)$, but the link bandwidth capacity is n^r for each link.

Definition 4: For an LAG $G_k^{sub}(V, E)$, the definition of the layered LRC (LaLRC) is as follows:

$$h_v^{(2)} = c_v \cdot \beta_v, \quad \forall v \in V \quad (15)$$

where β_v is the degree of the node v in the LAG G_k^{sub} .

³Note that this definition works for both the substrate network and the VON requests. For VON requests, the resource capacities should be replaced by the corresponding resource requirements.

Algorithm 2: Node Mapping

input : Substrate network G^s or $G_{k,j}^{sub}$, VON request G^r
output: VONE status F

- 1 calculate LRC or LaLRC and node degree β_{v^s} for each SN v^s in G^s or $G_{k,j}^{sub}$;
- 2 calculate LRC and node degree β_{v^r} for each VN v^r in G^r ;
- 3 **for all VNs v^r in descending order of their LRCs do**
- 4 $F = \text{FAILED}$;
- 5 **for all unmarked SNs v^s in descending order of their LRCs or LaLRCs do**
- 6 **if $c_{v^s}^s \geq c_{v^r}^r$ AND $\beta_{v^s} \geq \beta_{v^r}$ then**
- 7 map v^r onto v^s ;
- 8 mark v^s as selected;
- 9 $F = \text{SUCCEEDED}$;
- 10 **break**;
- 11 **end**
- 12 **end**
- 13 **if $F = \text{FAILED}$ then**
- 14 **return(F);**
- 15 **end**
- 16 **end**
- 17 **return(F);**

Algorithm 3: Link Mapping

input : Substrate network G_k^{sub} , VON request G^r
output: VONE status F

- 1 **for all VOLs $e^r = (u^r, v^r)$ in G^r do**
- 2 obtain the mapped SNs in G_k^{sub} for u^r and v^r ;
- 3 store the mapped SNs in u and v ;
- 4 find the shortest path from u to v in G_k^{sub} ;
- 5 **if the path cannot be found then**
- 6 **return($F = \text{FAILED}$);**
- 7 **end**
- 8 map $e^r = (u^r, v^r)$ onto the path;
- 9 remove all SFLs of the path in G_k^{sub} ;
- 10 **end**

Based on LRC or LaLRC, we design a greedy node mapping algorithm. We first calculate the LRC for each VN in the VON request, and then compute LRC for each SN in the substrate network G^s or the LaLRC for each SN in the connected component $G_{k,j}^{sub}$ of the LAG G_k^{sub} . The node mapping embeds the VN with the largest LRC onto the feasible SN that also has the largest LRC or LaLRC. *Algorithm 2* provides the details of the node mapping process.

3) *Link Mapping*: When all the VNs have been embedded successfully, we use the shortest-path routing for the link mapping. More specifically, the proposed link mapping algorithm sets up a lightpath in an LAG of the substrate network with the shortest-path routing for a VOL, and then removes the links in the lightpath from the LAG. Since the principle of constructing the LAG makes sure that both the routing path and the FS' on them are available for a VOL, we achieve integrated RSA. These procedures are done sequentially until the lightpaths of all VOLs have been set up successfully. *Algorithm 3* shows the detailed procedures of the link mapping.

4) *Overall VONE Algorithms*: Based on whether the heuristic utilizes the LRC in (14) or the LaLRC in (15) in the node mapping, we name them as *LRC-LaSP* and *LaLRC-layered shortest-*

Algorithm 4: LRC-LaSP Algorithm

input : Substrate network G^s , VON request G^r
output: VONE status F

- 1 $G_{temp}^s = G^s$;
- 2 apply *Algorithm 2* for node mapping;
- 3 **if node mapping is successful then**
- 4 **for $k = 1$ to $B^s - n^r + 1$ do**
- 5 build the k -th LAG G_k^{sub} with *Algorithm 1*;
- 6 apply *Algorithm 3* for link mapping;
- 7 **if link mapping is successful then**
- 8 provision G^r ;
- 9 **return($F = \text{SUCCEEDED}$);**
- 10 **end**
- 11 **end**
- 12 **end**
- 13 mark G^r as blocked;
- 14 $G^s = G_{temp}^s$;
- 15 **return($F = \text{FAILED}$);**

Algorithm 5: LaLRC-LaSP Algorithm

input : Substrate network G^s , VON request G^r
output: VONE status F

- 1 $G_{temp}^s = G^s$;
- 2 **for $k = 1$ to $B^s - n^r + 1$ do**
- 3 build the k -th LAG G_k^{sub} with *Algorithm 1*;
- 4 get all the connected components $G_{k,j}^{sub}$ of G_k^{sub} that have more or equal nodes than G^r ;
- 5 **for all $G_{k,j}^{sub}$ in the descending order of their node numbers do**
- 6 apply *Algorithm 2* for node mapping;
- 7 **if node mapping is successful then**
- 8 apply *Algorithm 3* for link mapping;
- 9 **if link mapping is successful then**
- 10 provision G^r ;
- 11 **return($F = \text{SUCCEEDED}$);**
- 12 **end**
- 13 **end**
- 14 **end**
- 15 **end**
- 16 mark G^r as blocked;
- 17 $G^s = G_{temp}^s$;
- 18 **return($F = \text{FAILED}$);**

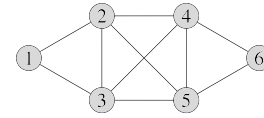


Fig. 3. Six-node topology.

path routing (LaSP), respectively. The terms before the hyphen indicate the algorithms' node mapping schemes, while the ones after are for their link mapping schemes. Here, LaSP stands for "layered shortest-path routing," since both algorithms rely on the LAG for integrated RSA in the link mapping. *Algorithms 4* and *5* show the overall procedures of the *LRC-LaSP* and *LaLRC-LaSP* algorithms, respectively.

C. Performance Evaluation of Transparent VONE

We design simulations to evaluate the performance of the proposed algorithms with three substrate network topologies, a simple six-node topology shown in Fig. 3, a realistic Deutsche Telecom (DT) topology with 14 nodes and 23 links [18] and a

TABLE I
SIMULATION PARAMETERS FOR TRANSPARENT VONE

	Six-Node Topology	DT Topology	Random Topology
Number of SNs	6	14	50
Number of SFLs	10	23	141
SN's Computing Capacity	50 units	200 units	200 units
SFL's Bandwidth Capacity	50 FS*	200 FS*	200 FS*
VN's Computing Requirement	[1, 3] units	[1, 10] units	[1, 20] units
VOL's Bandwidth Requirement	[1, 3] FS*	[1, 10] FS*	[1, 20] FS*
Number of VNs in a VON	[2, 3]	[3, 4]	[2, 10]

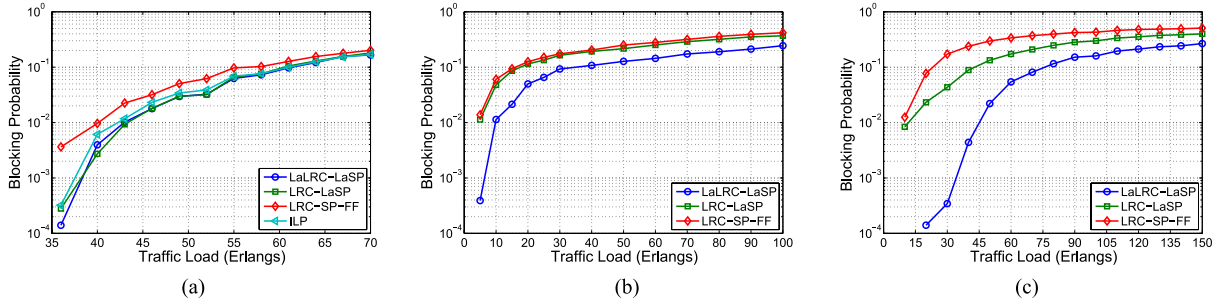


Fig. 4. Simulation results on request blocking probability for transparent VONE. (a) Six-node topology. (b) DT topology. (c) Random topology.

random topology with 50 nodes and 141 links that is generated using the GT-ITM tool [19]. For the six-node and the random topologies, we assume that the length of each SFL is identical as 100 km, and the SFLs in the DT topology have the same lengths as those in [18]. The VON requests are also generated using the GT-ITM tool. The number of VNs in each VON request is uniformly distributed in a preset range, and the probability that a VN-pair is directly connected equals 0.5, which means that there would be $\frac{n \cdot (n-1)}{4}$ VOLs on average for a VON request with n VNs. We consider dynamic VONE and generate the VON requests with the Poisson traffic model. The rest of the simulation parameters are in Table I.

1) *Benchmark Algorithm*: For the benchmark algorithm, we modify the algorithm in [17] and adapt it to VONE over EONs. Since the benchmark algorithm considers the LRC in the node mapping and utilizes the shortest-path routing and first-fit spectrum assignment for the link mapping, we name it as *LRC-SP-FF*.

2) *Performance Metrics*: We consider the request blocking probability, which is defined as the ratio of blocked to total arrived VON requests during the network operation, as the major performance metric. On the other hand, the lengths of substrate lightpaths can affect the quality of VONE, since the transmission delays and the PLIs depend on them [8]. Therefore, we also record the average length of the longest substrate lightpath per VON request.

3) *Simulation Results*: Fig. 4 shows the blocking probabilities obtained from the three topologies. We observe that among the algorithms, the benchmark algorithm, *LRC-SP-FF*, always provides the worst blocking performance. This observation verifies that the algorithms for VONE over EONs need special designs and they have to consider the spectrum utilization of substrate networks properly. Fig. 4(a) shows that the blocking performance of *LaLRC-LaSP*, *LRC-LaSP* and ILP is compa-

table, and ILP performs slightly worse than *LaLRC-LaSP* and *LRC-LaSP* for traffic loads lower than 50 Erlangs. Even though the ILP can get the optimal solution for each VON request and arrange the spectrum utilization in the most compact way for the time being, it is still a greedy algorithm from the perspective of overall network operation and cannot achieve the global optimum for all VON requests.

For the DT and random topologies, we skip the simulations with the ILP due to the high computational complexity. In Fig. 4(b) and (c), we can see that *LaLRC-LaSP* achieves the lowest blocking probability for all the cases. *LRC-LaSP* outperforms *LRC-SP-FF* in the random topology, while their block performance is comparable in the DT topology. These results suggest that the proposed LAG approach can improve the blocking performance, since it takes the information of spectrum utilization into consideration during VONE. Because *LaLRC-LaSP* involves LAG in both node mapping and link mapping, it achieves the best blocking performance.

Fig. 5 shows simulation results on the average length of the longest substrate light path per VON request. In Fig. 5(a), we observe that the ILP provides the shortest lengths for all the cases in the six-node topology. Since the results are all around 100 km, we can conclude that the ILP manages to map most of the VOLs onto substrate lightpaths that only have one hop. The results from *LaLRC-LaSP* are the second shortest, while those from *LRC-LaSP* are the longest. In Figs. 5(b) and (c), we can still see that results from *LRC-LaSP* are the longest. This phenomenon can be explained as follows. Without the LAG approach, the node mapping in *LRC-LaSP* can deviate much from the optimum, while due to spectrum unavailability, its subsequent link mapping with LAG may not select the shortest substrate lightpath. Therefore, these two negative factors add up and cause *LRC-LaSP* to provide the longest average maximum lengths.

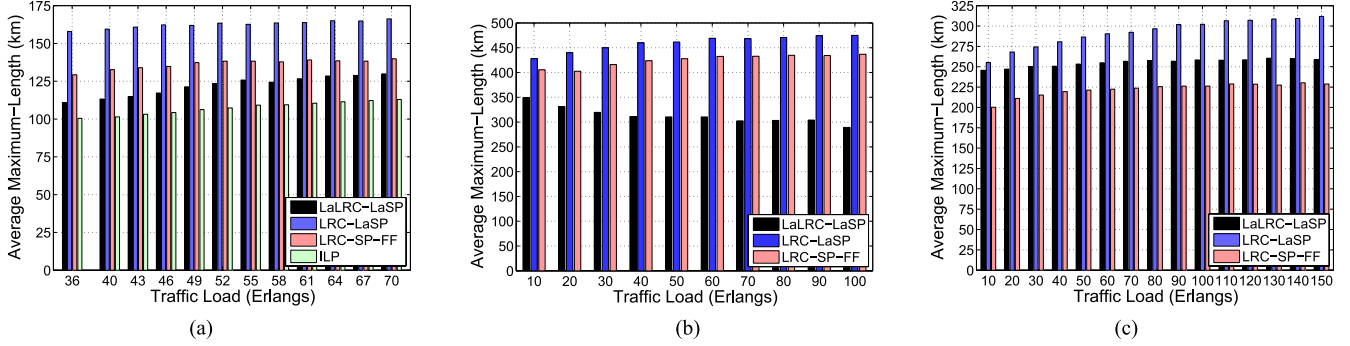


Fig. 5. Simulation results on average length of the longest substrate lightpath per VON request for transparent VONE. (a) Six-node topology. (b) DT topology. (c) Random topology.

In Fig. 5(c), it is interesting to notice that the lengths from the benchmark algorithm, *LRC-SP-FF*, are shorter than those from *LaLRC-LaSP*. Since *LRC-SP-FF* does not make full use of the information of spectrum utilization, it does not consider the spectrum continuity in the node mapping and always selects the shortest substrate lightpath for the link mapping regardless of its spectrum utilization. Therefore, in a relatively large topology as the random topology, *LRC-SP-FF* can provide shorter lengths of the substrate light paths. Meanwhile, it can also cause more congestions on certain links easily. The rationale can be verified with the blocking performance in Fig. 4(c), where *LRC-LaSP* achieves much lower blocking probability than *LRC-SP-FF*.

V. OPAQUE VONE OVER EONS

A. ILP Formulation

In this section, we develop a path-based ILP formulation for the opaque VONE over EONS. Initially, for each node pair in the substrate network $G^s(V^s, E^s)$, by using Yen's K-shortest path algorithm [20], we calculate K shortest paths whose transmission distances are within the maximum transmission reach of the lowest possible modulation-level⁴. Note that for the opaque VONE, we consider the case that the substrate lightpath can select its modulation-level adaptively from BPSK, QPSK, 8QAM, and 16QAM according to the transmission distance (i.e., the PLIs) [21]. We assume that the bandwidth of one FS is 12.5 GHz and it can carry $C_{FS} = 12.5$ Gb/s signal when the modulation-level is BPSK. Based on the experimental results in [21] and [22], we set the transmission reach of BPSK, QPSK, 8QAM, and 16QAM signals as 3000, 1500, 750, and 375 km, respectively, and therefore the maximum transmission reach of the lowest possible modulation-level, BPSK, is 3000 km. When the transmission distance of a VOL's substrate lightpath permits, we always select the highest possible modulation level for it for the highest spectral efficiency [23], [24]. Hence, for all the precalculated substrate routing paths, their modulation-levels to use are also predetermined. The ILP formulation is as follows⁵.

Parameters:

⁴Note that, if we cannot find K paths that are within the maximum transmission reach, we just use all feasible paths.

⁵Note that the parameters and variables that are the same as those in the ILP formulation of the transparent VONE are omitted here.

- 1) P^s Set of all the precalculated routing paths in the substrate network $G^s(V^s, E^s)$.
- 2) $s_{p^s}^s$ Source node of the path $p^s \in P^s$.
- 3) $d_{p^s}^s$ Destination node of the path $p^s \in P^s$.
- 4) $P_{e^s}^s$: Set of the routing paths that use the SFL e^s , obviously, $P_{e^s}^s \subset P^s$.
- 5) $m_{p^s}^s$ Highest modulation-level for the path p^s .
- 6) $bw_{e^r}^r$ Bandwidth requirement of the VOL e^r in the VON request $G^r(V^r, E^r)$.
- 7) $w_{e^s, k}^s$ Starting FS index of the k th MCSB on SFL e^s .
- 8) $z_{e^s, k}^s$ Ending FS index of the k th MCSB on SFL e^s .

Variables:

- 1) ζ_{e^r, p^s} Boolean variable that equals 1, if a VOL e^r is mapped onto the substrate lightpath p^s , otherwise, it is 0.
- 2) π_{e^r, e^s} Boolean variable that equals 1, if a VOL e^r uses the SFL e^s , otherwise, it is 0.
- 3) $\sigma_{e_1^r, e_2^r}$ Boolean variable that equals 1, if two VOLs e_1^r and e_2^r use common SFL(s), otherwise, it is 0.
- 4) $\rho_{e_1^r, e_2^r}$ Boolean variable that equals 1, if the starting FS index of the assigned CSB of the VOL e_1^r is smaller than that of the VOL e_2^r , otherwise, it is 0.
- 5) w_{e^r} Integer variable that indicates the starting FS index of the assigned CSB for VOL e^r .
- 6) z_{e^r} Integer variable that indicates the ending FS index of the assigned CSB for VOL e^r .
- 7) $\delta_{e^r, e^s}^{(k)}$ Boolean variable that equals 1, if the k th MCSB on an SFL e^s is selected to serve the VOL e^r , otherwise, it is 0.

Objective:

$$\text{Minimize } \sum_{e^r \in E^r} \sum_{p^s \in P^s} \zeta_{e^r, p^s} \cdot |p^s| \cdot \left\lceil \frac{bw_{e^r}^r}{m_{p^s}^s \cdot C_{FS}} \right\rceil \quad (16)$$

where $C_{FS} = 12.5$ Gb/s is the capacity of one FS when the modulation level is BPSK, $|p^s|$ returns the hop count of p^s , and $m_{p^s}^s$ is the modulation-level for p^s , which equals to 1, 2, 3, and 4, for BPSK, QPSK, 8QAM, and 16QAM, respectively. The term $\left\lceil \frac{bw_{e^r}^r}{m_{p^s}^s \cdot C_{FS}} \right\rceil$ calculates the number of FS' that we need to allocate to VOL e^r , when it is mapped onto the substrate light path p^s . The objective in (16) aims to minimizing the total number of assigned FS' for the VON request.

Constraints:

1) Node mapping,

The node mapping constraints are the same as those in the transparent VONE.

2) Link mapping,

$$\zeta_{e^r, p^s} \leq \xi_{s_{e^r}^r, s_{p^s}^s}, \quad \forall e^r \in E^r, \forall p^s \in P^s \quad (17)$$

$$\zeta_{e^r, p^s} \leq \xi_{d_{e^r}^r, d_{p^s}^s}, \quad \forall e^r \in E^r, \forall p^s \in P^s \quad (18)$$

$$\sum_{p^s \in P^s} \zeta_{e^r, p^s} = 1, \quad \forall e^r \in E^r \quad (19)$$

$$\sum_{e^r \in E^r} \zeta_{e^r, p^s} \leq 1, \quad \forall p^s \in P^s. \quad (20)$$

Equations (17)–(20) ensure that each VOL is mapped onto a single substrate lightpath, and the end nodes of the lightpath are the embedded SNs that the corresponding VNs are mapped onto,

$$\sigma_{e_1^r, e_2^r} \geq \zeta_{e_1^r, p_1^s} + \zeta_{e_2^r, p_2^s} - 1, \quad \forall e_1^r, e_2^r \in E^r, \forall p_1^s, p_2^s \in P^s \quad (21)$$

$$\rho_{e_1^r, e_2^r} + \rho_{e_2^r, e_1^r} = 1, \quad \forall e_1^r, e_2^r \in E^r \quad (22)$$

$$z_{e_2^r} - w_{e_1^r} + 1 \leq B^s \cdot (1 + \rho_{e_1^r, e_2^r} - \sigma_{e_1^r, e_2^r}), \quad \forall e_1^r, e_2^r \in E^r \quad (23)$$

$$z_{e_1^r} - w_{e_2^r} + 1 \leq B^s \cdot (2 - \rho_{e_1^r, e_2^r} - \sigma_{e_1^r, e_2^r}), \quad \forall e_1^r, e_2^r \in E^r. \quad (24)$$

Equations (21)–(24) together with (26)–(29) ensure that the spectrum assigned to any VOL is contiguous and the spectra assigned to any two VOLs whose substrate lightpaths have common SFL(s) do not overlap,

$$z_{e^r} - w_{e^r} + 1 = \sum_{p^s \in P^s} \zeta_{e^r, p^s} \cdot \left\lceil \frac{bw_{e^r}^r}{m_{p^s}^s \cdot C_{FS}} \right\rceil, \quad \forall e^r \in E^r \quad (25)$$

Equation (25) ensures that the number of FS' assigned to each VOL can satisfy its bandwidth requirement:

$$\pi_{e^r, e^s} \geq \zeta_{e^r, p^s}, \quad \forall e^r \in E^r, \forall e^s \in E^s, \forall p^s \in P^s \quad (26)$$

$$\sum_k \delta_{e^r, e^s}^{(k)} = \pi_{e^r, e^s}, \quad \forall e^r \in E^r, \forall e^s \in E^s \quad (27)$$

$$w_{e^r} \geq w_{e^s, k}^s \cdot (\delta_{e^r, e^s}^{(k)} + \pi_{e^r, e^s} - 1), \quad \forall e^r \in E^r, \forall e^s \in E^s, \forall k \quad (28)$$

$$z_{e^r} - z_{e^s, k}^s \leq B^s \cdot (2 - \delta_{e^r, e^s}^{(k)} - \pi_{e^r, e^s}), \quad \forall e^r \in E^r \quad (29)$$

$$\forall e^s \in E^s, \forall k.$$

Equations (26)–(29) ensure that the assigned CSB for each VOL in the VON request locates in a single MCSB on SFL e^s , and the MCSB's size is not smaller than that of the assigned CSB.

Variable range,

$$\pi_{e^r, e^s}, \delta_{e^r, e^s}^{(k)} \in \{0, 1\}, \quad \forall e^r \in E^r, \forall e^s \in E^s, \forall k \quad (30)$$

$$\zeta_{e^r, p^s} \in \{0, 1\}, \quad \forall e^r \in E^r, \forall p^s \in P^s \quad (31)$$

$$\sigma_{e_1^r, e_2^r}, \rho_{e_1^r, e_2^r} \in \{0, 1\}, \quad \forall e_1^r, e_2^r \in E^r \quad (32)$$

$$w_{e^r}, z_{e^r} \in [1, B^s], \quad e^r \in E^r. \quad (33)$$

Equations (30)–(33) limit the ranges of the variables.

B. Heuristic Algorithm

Due to its computational complexity, solving the ILP may not be suitable for online opaque VONE. Therefore, we propose an efficient heuristic algorithm that considers the spectrum consecutiveness during the opaque VONE. The proposed algorithm consists of two stages, node mapping and link mapping. The node mapping utilizes a consecutiveness-aware LRC, and the link mapping is based on K shortest-path routing and first-fit spectrum assignment.

1) *Consecutiveness-Aware LRC:* For the opaque VONE, we design a consecutiveness-aware LRC (CaLRC) that considers the spectrum consecutiveness of each SFL.

Definition 5: For a substrate network $G^s(V^s, E^s)$, the definition of the CaLRC is as follows:

$$h_{v^s}^{(3)} = c_{v^s}^s \cdot \sum_{(v^s, u^s) \in E^s} q_{(v^s, u^s)}, \quad \forall v^s \in V^s \quad (34)$$

where $q_{(v^s, u^s)}$ is the spectrum consecutiveness of the SFL (v^s, u^s) , which is modified from the definition in [25] as

$$q_{e^s} = \sum_k \sum_{i=1}^{n_{e^s}^{(k)}} (n_{e^s}^{(k)} - i + 1) \cdot \alpha_i, \quad \forall e^s = (v^s, u^s) \in E^s \quad (35)$$

where $n_{e^s}^{(k)} = z_{e^s, k}^s - w_{e^s, k}^s + 1$ is the size of the k th MCSB on SFL e^s in terms of FS', and α_i is the weight coefficient for the CSB that has a size of i FS',

$$\alpha_i = \begin{cases} 1, & i \in N^r \\ 0, & \text{otherwise} \end{cases} \quad (36)$$

where N^r is the set of all the possible numbers of FS' required by the VON request.

2) *Overall VONE Algorithm:* With CaLRC, the node mapping is done as follows, whenever the VN's computing resource requirement can be satisfied, we map the VN with the largest LRC onto the unmarked SN that has the largest CaLRC. In the link mapping, the VOLs are first sorted based on their bandwidth requirements in descending order, and RSA is performed for each VOL with the K shortest-path (KSP) routing and first-fit (FF) spectrum assignment. *Algorithm 6* illustrates the proposed *CaLRC-KSP-FF* algorithm.

Leftleft Thisthis Upup UnionUnion FindCompressFindCompress Inputinput Outputoutput VONE status F

```

 $G_{temp}^s = G^s$ 
calculate CaLRC for each SN  $v^s$  in  $G^s$ 
calculate LRC for each VN  $v^r$  in  $G^r$ 
all  $v^r$  in descending order of LRCs  $F = \text{FAILED}$ 
all unmarked  $v^s$  in descending order of CaLRCs  $c_{v^s}^s \geq c_{v^r}^r$ 
map  $v^r$  onto  $v^s$ 
mark  $v^s$  as selected
 $F = \text{SUCCEEDED}$ 
break  $F = \text{FAILED}$  mark  $G^r$  as blocked

```

TABLE II
SIMULATION PARAMETERS FOR OPAQUE VONE

	Six-Node Topology	DT Topology	Random Topology
K , number of routing-paths between each SN-pair	3	10	10
VN's Computing Capacity Requirement	[1, 4] units	[1, 6] units	[1, 6] units
VOL's Bandwidth Requirement	[12.5, 150] Gb/s	[12.5, 125] Gb/s	[12.5, 250] Gb/s
Number of VNs in a VON	[2, 3]	[2, 7]	[2, 10]

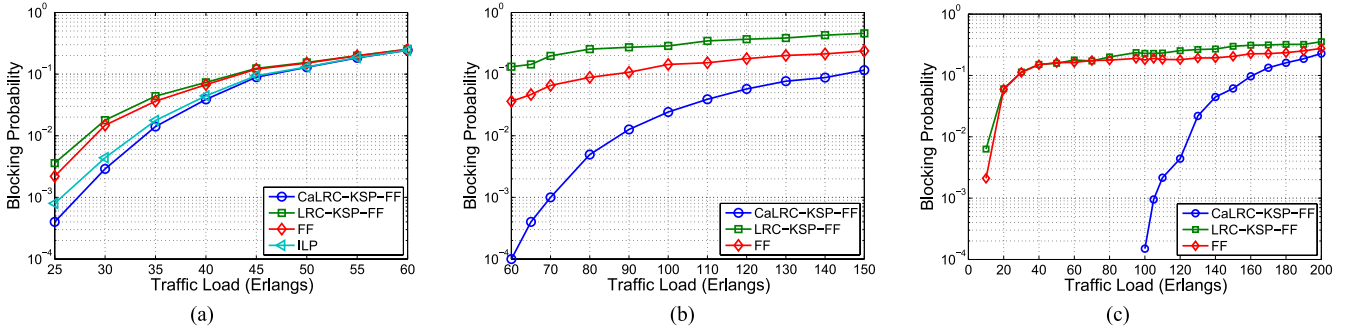


Fig. 6. Simulation results on request blocking probability for opaque VONE. (a) Six-node topology. (b) DT topology. (c) Random topology.

Algorithm 6: *CaLRC-KSP-FF* Algorithm

```

input : Substrate network  $G^s$ , VON request  $G^r$ 
output: VONE status  $F$ 
1  $G_{temp}^s = G^s$ ;
2 calculate CaLRC for each SN  $v^s$  in  $G^s$ ;
3 calculate LRC for each VN  $v^r$  in  $G^r$ ;
4 for all  $v^r$  in descending order of LRCs do
5    $F = \text{FAILED}$ ;
6   for all unmarked  $v^s$  in descending order of
   CaLRCs do
7     if  $c_{v^s}^s \geq c_{v^r}^r$  then
8       map  $v^r$  onto  $v^s$ ;
9       mark  $v^s$  as selected;
10       $F = \text{SUCCEEDED}$ ;
11      break;
12     end
13   end
14   if  $F = \text{FAILED}$  then
15     mark  $G^r$  as blocked;
16      $G^s = G_{temp}^s$ ;
17     return( $F$ );
18   end
19 end
20 for all  $e^r$  in descending order of  $bw_{e^r}^r$  do
21    $F = \text{FAILED}$ ;
22   for  $k = 1$  to  $K$  do
23     perform link mapping for  $e^r$  with the  $k$ -th
     shortest path  $p_k$  between the two embedded
     SNs for the end-nodes of  $e^r$ ;
24     if link mapping is successful then
25        $F = \text{SUCCEEDED}$ ;
26       break;
27     else
28       mark  $G^r$  as blocked;
29        $G^s = G_{temp}^s$ ;
30       return( $F$ );
31     end
32   end
33 end
34 return( $F$ );

```

$$G^s = G_{temp}^s$$

return (F)

all e^r in descending order of $bw_{e^r}^r$ $F = \text{FAILED}$

$k = 1$ to K

perform link mapping for e^r with the k th shortest path p_k between the two embedded SNs for the end-nodes of e^r

link mapping is successful

$F = \text{SUCCEEDED}$

break

mark G^r as blocked

$$G^s = G_{temp}^s$$

return (F)

return (F)

CaLRC-KSP-FF Algorithm

C. Performance Evaluation of Opaque VONE

We evaluate the performance of the proposed opaque VONE algorithms with the similar simulation setup as that in Section IV-C. The new/different simulation parameters are summarized in Table II. For the benchmark algorithms, we use *LRC-KSP-FF* and *FF*. *LRC-KSP-FF* is similar to *LRC-SP-FF* with the only difference that each SN-pair has K shortest routing paths for the link mapping. *FF* is modified from the FF algorithm proposed in [11]⁶, which embeds each VN onto the first SN that has enough computing resources and then applies the K -shortest-paths based link mapping. Note that in our implementation, we do not allow FF to embed different VNs in the same VON request onto the same SN.

⁶Note that in [11], the authors also proposed a link-list (LL) VONE algorithm. However, for embedding each VOL, LL needs to evaluate all the possible substrate light paths. In our case, this means that we may need to evaluate $\frac{|V^s|(|V^s|-1)}{2}$. K substrate light paths for embedding a VOL. The computational complexity of LL is too high for our case

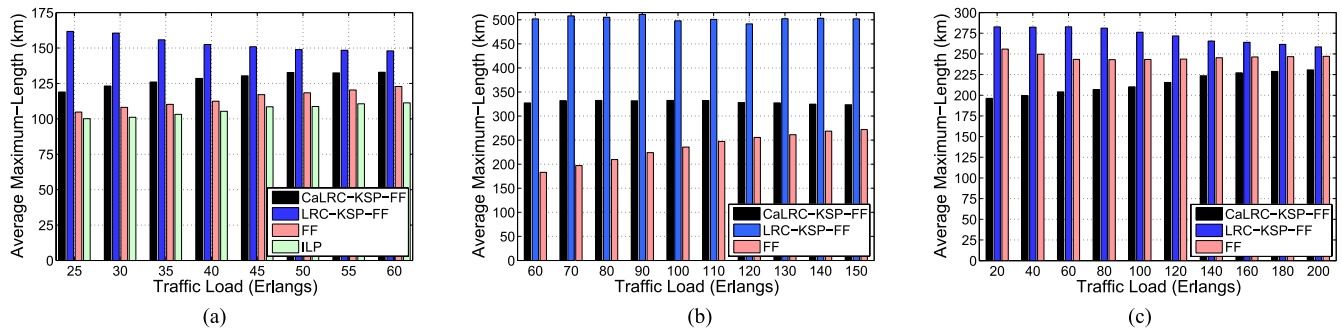


Fig. 7. Simulation results on average length of the longest substrate lightpath per VON request for opaque VONE. (a) Six-node topology. (b) DT topology. (c) Random topology.

1) *Simulation Results:* Fig. 6 illustrates the simulation results on the blocking probability. We can see that *CaLRC-KSP-FF* achieves the best blocking performance for all the cases, and its blocking performance is slightly better than that of ILP in the six-node topology. This is because *CaLRC-KSP-FF* consider the spectrum consecutiveness of each SFL properly during VONE. The blocking performance of FF is comparable with *LRC-KSP-FF* in the six-node and random topologies, while in the DT topology, *FF* outperforms *LRC-KSP-FF* significantly. Fig. 7 shows the results on the average length of the longest substrate light path per VON request. FF provides shorter results than *CaLRC-KSP-FF* in the six-node and DT topologies, but in the random topology, its results are longer than those from *CaLRC-KSP-FF*.

VI. CONCLUSION

In this paper, we studied algorithms for both transparent and opaque VONE over EONs. For transparent VONE, we first formulated an ILP model that leveraged the all-or-nothing multi-commodity flow in graphs. Then, to consider the continuity and consecutiveness of SFLs' optical spectra, we proposed a LAG approach that decomposed the physical infrastructure into several layered graphs according to the bandwidth requirement of a VON request. With this approach, we designed two heuristic algorithms: one applies LAG to achieve integrated RSA in link mapping (i.e., *LRC-LaSP*), while the other realizes coordinated node and link mapping using LAG (i.e., *LaLRC-LaSP*). The simulation results from three different substrate topologies demonstrated that *LaLRC-LaSP* achieved better blocking performance than *LRC-LaSP* and an existing benchmark algorithm. For the opaque VONE, an ILP model was also formulated. We then designed a LRC metric that considered the spectrum consecutiveness of SFLs. With this metric, a novel heuristic for opaque VONE, *CaLRC-KSP-FF*, was proposed. Simulation results showed that compared with the existing algorithms, *CaLRC-KSP-FF* could reduce the request blocking probability significantly.

REFERENCES

- [1] A. Wang, M. Iyer, R. Dutta, G. Rouskas, and I. Baldine, "Network virtualization: Technologies, perspectives, and frontiers," *J. Lightw. Technol.*, vol. 31, no. 4, pp. 523–537, Feb. 2013.
- [2] O. Gerstel, M. Jinno, A. Lord, and B. Yoo, "Elastic optical networking: A new dawn for the optical layer?" *IEEE Commun. Mag.*, vol. 50, no. 2, pp. S12–S20, Feb. 2012.
- [3] R. Nejabati, E. Escalona, S. Peng, and D. Simeonidou, "Optical network virtualization," in *Proc. Int. Conf. Opt. Netw. Des. Model.*, Feb. 2011, pp. 1–5.
- [4] M. Jinno, "Virtualization in optical networks: From elastic networking level to sliceable equipment level," in *Proc. Int. Conf. Opt. Internet*, May 2012, pp. 61–62.
- [5] S. Figuerola and M. Lemay, "Infrastructure services for optical networks," *J. Opt. Commun. Netw.*, vol. 1, pp. A247–A257, Jul. 2009.
- [6] A. Pages, J. Perello, and S. Spadaro, "Virtual network embedding in optical infrastructures," in *Proc. Int. Conf. Transparent Opt. Netw.*, Jul. 2012, pp. 1–4.
- [7] S. Zhang, L. Shi, C. Vadrevu, and B. Mukherjee, "Network virtualization over WDM networks," in *Proc. Int. Conf. Adv. Netw. Telecommun. Syst.*, Dec. 2011, pp. 1–3.
- [8] S. Peng, R. Nejabati, S. Azodolmolky, E. Escalona, and D. Simeonidou, "An impairment-aware virtual optical network composition mechanism for future Internet," *Opt. Exp.*, vol. 19, pp. B251–B259, Dec. 2011.
- [9] Q. Zhang, W. Xie, Q. She, X. Wang, P. Palacharla, and M. Sekiya, "RWA for network virtualization in optical WDM networks," in *Proc. Opt. Fiber Commun. Conf. Expo.*, Mar. 2013, pp. 1–3.
- [10] A. Pages, J. Perello, S. Spadaro, J. Garcia-Espin, J. Ferrer Riera, and S. Figuerola, "Optimal allocation of virtual optical networks for the future Internet," in *Proc. Int. Conf. Opt. Netw. Des. Model.*, Apr. 2012, pp. 1–6.
- [11] J. Zhang, S. Subramaniam, and M. Brandt-Pearce, "Virtual topology mapping in elastic optical networks," in *Proc. Int. Conf. Commun.*, Jun., pp. 1–5.
- [12] L. Gong, W. Zhao, Y. Wen, and Z. Zhu, "Dynamic transparent virtual network embedding over elastic optical infrastructures," in *Proc. Int. Conf. Commun.*, Jun. 2013, pp. 1–5.
- [13] A. Fischer, J. Botero, M. Beck, H. De Meer, and X. Hesselbach, "Virtual network embedding: A survey," *IEEE Commun. Surveys Tuts.*, vol. 15, no. 4, pp. 1888–1906, 2013.
- [14] A. Belbekkouche, M. Hasan, and A. Karmouch, "Resource discovery and allocation in network virtualization," *IEEE Commun. Surveys Tuts.*, vol. 14, no. 4, pp. 1114–1128, Oct./Dec. 2012.
- [15] L. Gong, X. Zhou, W. Lu, and Z. Zhu, "A two-population based evolutionary approach for optimizing routing, modulation and spectrum assignments (RMSA) in O-OFDM networks," *IEEE Commun. Lett.*, vol. 16, no. 9, pp. 1520–1523, Sep. 2012.
- [16] R. Ahuja, T. Magnanti, and J. Orlin, *Network Flows: Theory, Algorithms, and Applications*. Englewood Cliffs, NJ, USA: Prentice-Hall, 1993.
- [17] M. Yu, Y. Yi, J. Rexford, and M. Chiang, "Rethinking virtual network embedding: Substrate support for path splitting and migration," *SIGCOMM Comput. Commun. Rev.*, vol. 28, pp. 17–29, Feb. 2008.
- [18] S. Azodolmolky *et al.*, "Experimental demonstration of an impairment aware network planning and operation tool for transparent/translucent optical networks," *J. Lightw. Technol.*, vol. 29, no. 4, pp. 439–448, Feb. 2011.
- [19] E. Zegura, K. Calvert, and S. Bhattacharjee, "How to model an internet network," in *Proc. IEEE Conf. Comput. Commun.*, Mar. 1996, pp. 594–602.
- [20] J. Yen, "Finding the K shortest loopless paths in a network," *Manag. Sci.*, vol. 17, pp. 712–716, 1971.

- [21] A. Bocoi, M. Schuster, F. Rambach, M. Kiese, C. Bunge, and B. Spinnler, "Reach-dependent capacity in optical networks enabled by OFDM," in *Proc. Conf. Opt. Fiber Commun.*, Mar. 2009, pp. 1–3.
- [22] M. Jinno, B. Koziicki, H. Takara, A. Watanabe, Y. Sone, T. Tanaka, and A. Hirano, "Distance-adaptive spectrum resource allocation in spectrum-sliced elastic optical path network," *IEEE Commun. Mag.*, vol. 48, no. 8, pp. 138–145, Aug. 2010.
- [23] W. Lu and Z. Zhu, "Dynamic service provisioning of advance reservation requests in elastic optical networks," *J. Lightw. Technol.*, vol. 31, no. 10, pp. 1621–1627, May 2013.
- [24] L. Gong, X. Zhou, X. Liu, W. Zhao, W. Lu, and Z. Zhu, "Efficient resource allocation for all-optical multicasting over spectrum-sliced elastic optical networks," *J. Opt. Commun. Netw.*, vol. 5, pp. 836–847, Aug. 2013.
- [25] Y. Sone, A. Hirano, A. Kadohata, M. Jinno, and O. Ishida, "Routing and spectrum assignment algorithm maximizes spectrum utilization in optical networks," in *Proc. Eur. Conf. Exhib. Opt. Commun.*, Sep. 2011, pp. 1–3.

Long Gong (S'11) received the B.S. degree from the School of Information Science and Technology, University of Science and Technology of China (USTC), Hefei, China. He is working toward the M.S. degree at USTC. His research interest is elastic optical networks.

Zuqing Zhu (M'07–SM'12) received the Ph.D. degree from the Department of Electrical and Computer Engineering, University of California, Davis, USA, in 2007. From July 2007 to January 2011, he worked in the Service Provider Technology Group of Cisco Systems, San Jose, as a senior R&D engineer. In January 2011, he joined the University of Science and Technology of China (USTC), where he currently is an Associate Professor. He has published more than 100 papers in peer-reviewed journals and conferences. He has been in the technical program committees (TPC) of INFOCOM, ICC, GLOBECOM, ICCCN and etc. He is also an editorial board member of Elsevier *Journal of Optical Switching and Networking*, Springer *Telecommunication Systems Journal*, Wiley *European Transactions on Emerging Telecommunications Technologies*, and etc. Dr. Zhu received the Best Paper Awards from the IEEE International Conference on Communications (ICC) 2013 and the IEEE Global Communications Conference (GLOBECOM) 2013. He is a Senior Member of OSA.